Proc. Natl. Acad. Sci. USA
Vol. 82, pp. 2287–2291, April 1985
Biochemistry

c-*erbB* activation in avian leukosis virus-induced erythroblastosis: Clustered integration sites and the arrangement of provirus in the c-*erbB* alleles

(retrovirus/cellular oncogene/epidermal growth factor receptor/promoter insertion)

MARIBETH A. RAINES*†, WYNNE G. LEWIS*, LYMAN B. CRITTENDEN‡, AND HSING-JIEN KUNG*†§

*Department of Biochemistry, Michigan State University, East Lansing, MI 48824; and ‡U.S. Department of Agriculture, Regional Poultry Research Laboratory, East Lansing, MI 48823

Communicated by Charles J. Arntzen, December 6, 1984

ABSTRACT **There is considerable evidence that links the activation of cellular genes to oncogenesis. We previously reported that structural rearrangements in the cellular oncogene c-*erbB* correlate with the development of erythroblastosis induced by avian leukosis virus (ALV). c-*erbB* recently has been shown to be related to the gene encoding epidermal growth factor receptor. We now have characterized the detailed mechanisms of c-*erbB* activation by ALV proviruses. We report here that the ALV proviral integration sites are clustered 5′ to the region where homology to v-*erbB* starts, suggesting that interruption in this region of c-*erbB* is important for its activation. The proviruses are oriented in the same transcriptional direction as c-*erbB* and usually are full-size. The latter finding is in contrast to the frequent deletions observed within the c-*myc*-linked proviruses in B-cell lymphomas. We have also identified a second c-*erbB* allele, which differs from the previously known allele primarily by a deletion in an intron region. This allele is also oncogenic upon mutation by an ALV provirus.**

Avian leukosis virus (ALV), a naturally occurring cancer virus of chickens, can induce a variety of neoplasms, including B-cell lymphomas, erythroblastosis, nephroblastomas, fibrosarcomas, etc. (1, 2). In the past few years, the mechanisms of ALV oncogenesis have been characterized in some detail (3–8). It was shown that ALV induces B-lymphomas by activation of the host oncogene c-*myc* (3). This activation of c-*myc* is accomplished by the insertion of an ALV provirus, which carries strong promoter/enhancer sequences, near the c-*myc* gene. We recently reported evidence suggesting that ALV induces erythroblastosis by a similar mechanism, with proviruses inserted near another host oncogene, c-*erbB* (9). c-*erbB* is the cellular homolog of one of the oncogenes carried by avian erythroblastosis virus (AEV), an acute oncogenic retrovirus known to induce rapid erythroblastosis in chickens (1, 10). The data indicate that, upon activation, c-*erbB* can assume an oncogenic role similar to that of its viral counterpart. In our previous communication, we showed a strong correlation between ALV-induced structural alterations of the c-*erbB* gene and the development of erythroblastosis (9). No alteration of c-*erbA* (the cellular homolog of the other oncogene of AEV) was found in any of the samples analyzed. Furthermore, in all the leukemic samples analyzed to date, transcription of c-*erbB* but not c-*erbA* is highly elevated (unpublished data). The data suggest that activation of the c-*erbB* gene alone is sufficient to cause erythroblast transformation. Although these studies provided important insights into the involvement of the c-*erbB* locus in the development of erythroblastosis, little was known about its activation mechanism, since the position, orientation, and structure of the adjoining ALV proviruses had not been examined. In addition, the c-*erbB* gene appeared to be more complex than previously reported. Using restriction endonuclease analysis, we had detected polymorphism in the c-*erbB* locus, a feature atypical of most cellular oncogenes. At least seven different *Eco*RI-digestion patterns of c-*erbB* were identified (ref. 9 and unpublished data). Several of the *erbB*-related fragments could not be accounted for by the published map of c-*erbB* (10). The nature of these polymorphic elements—whether they represented different alleles, members of a gene family, or pseudogenes—had not been explored.

We report here our detailed characterization of an additional 37 erythroblastosis samples induced in line 15_1 chicks by ALV infection. Our data may be summarized as follows: (*i*) A 100% correlation of c-*erbB* structural alteration with the development of erythroblastosis was observed. The great majority of the proviral integration sites are clustered in a region at the 5′ end of the first exon homologous to v-*erbB*, suggesting that disruption of the c-*erbB* locus in this region is important for its activation. (*ii*) Most of the proviruses appear to be full-length and oriented in the same transcriptional direction as c-*erbB*. One such provirus was molecularly cloned and shown to be completely intact. This finding contrasts with the analogous studies with B-lymphomas, where c-*myc*-linked proviruses usually carry large deletions. (*iii*) A second c-*erbB* allele was identified. This allele is also potentially oncogenic and can be mutated by an ALV provirus to cause erythroblastosis.

MATERIALS AND METHODS

Collection and Analysis of Erythroleukemic Samples. RAV-1, a prototype ALV, was used to inoculate 1-day-old line 15_1 chicks. The development of erythroblastosis and collection of leukemic samples were similar to those described previously (9).

DNA was extracted from quick-frozen bone marrow or liver samples as described by Maniatis *et al.* (11). DNA samples (25 μg) were digested with restriction enzymes under conditions recommended by the supplier (Bethesda Research Laboratories). Digested DNAs were ethanol-precipitated, dissolved in 10 mM Tris Cl, pH 8.0/1 mM EDTA, and then electrophoresed in 0.7% agarose gel, transferred to nitrocellulose, and hybridized with the appropriate radioactive probes (9, 11).

The publication costs of this article were defrayed in part by page charge payment. This article must therefore be hereby marked "*advertisement*" in accordance with 18 U.S.C. §1734 solely to indicate this fact.

Abbreviations: ALV, avian leukosis virus; AEV, avian erythroblastosis virus; LTR, long terminal repeat; EGF, epidermal growth factor; kb, kilobase(s).

†Present address: Department of Molecular Biology and Microbiology, Case Western Reserve University, Cleveland, OH 44106.
§To whom reprint requests should be addressed.

Radioactive Probes and Molecular Hybridization. All restriction fragments were purified by agarose gel electrophoresis and electroelution prior to radiolabeling (11). Hybridization probes were synthesized from the isolated DNA fragments by nick-translation, and hybridizations were carried out under conditions identical to those previously reported (9). Filters were washed in 30 mM NaCl/3 mM sodium citrate, pH 7/0.1% $NaDodSO_4$ at 65°C, dried, and exposed to x-ray film.

Molecular Cloning and Restriction-Enzyme Mapping. Partial *Eco*RI digests of liver DNA were size-selected on sucrose density gradients and ligated to the arms of phage vector EMBL-4 (12). The recombinant phages were packaged and screened by probes specific for v-*erbB* and the ALV long terminal repeat (LTR) as described (11, 13). Restriction-enzyme mapping of recombinants was performed by single and double digestions, followed by Southern blot (14) analysis with ALV- and v-*erbB*-specific probes.

RESULTS

α and β Alleles of c-*erbB*. Vennstrom and Bishop (10) previously have isolated and characterized c-*erbB* clones, derived from a genomic library of an outbred Leghorn chicken. The *Eco*RI and exon maps at this allele, designated the α allele of c-*erbB*, are shown in Fig. 1*A*. Our subsequent studies revealed restriction-fragment polymorphisms of c-*erbB* in different inbred lines of chickens (9). The most obvious difference is the presence of the 4.5- and 12.0-kilobase (kb) *Eco*RI fragments in some birds and the presence of the 2.3-, 5.3-, and 6.4-kb *Eco*RI fragments in others. By cloning and fine-structure mapping, we now have identified a second c-*erbB* allele, β, that can adequately account for these polymorphic variations (data to be published elsewhere). The *Eco*RI map of the β allele is summarized in Fig. 1*A*. The major difference between α and β lies in the intron region next to VB1, the first exon homologous to v-*erbB*. The β allele has a deletion of ≈2.5 kb in this region, with the appearance of a new *Eco*RI site near the boundary of this deletion. An additional *Eco*RI site specific for the β allele is located further downstream and splits the 12-kb fragment present in the α allele into 5.3- and 6.4-kb fragments. Aside from these two differences, the α and β alleles are very much alike. Neither of the polymorphic variations seems to affect the coding region of c-*erbB*, although conclusive evidence awaits the direct DNA sequence comparison of the two alleles. In an extensive survey of the inbred chickens maintained at the United States Department of Agriculture Regional Poultry Research Laboratory, we found that most lines (e.g., $15I_5$, 15_B, 7, and 6_3) carry α alleles. β alleles were identified in line 15_1 and RLC (and in K28; H. Robinson, personal communication). Among the 15_1 birds surveyed, 65% are homozygous for α, 10% are homozygous for β, and the remaining 25% are heterozygous for α and β.

Activation of the α Allele by ALV Proviral Insertion. We previously have shown that a c-*erbB* structural alteration correlates with the development of erythroblastosis (9). One fragment from an altered c-*erbB* locus was molecularly cloned, and it was shown by direct sequencing that the alteration is due to the insertion of an ALV LTR about 1.6 kb upstream from the VB1 exon. To determine whether LTR insertion near the VB1 exon is a general activation mechanism, we have analyzed 37 additional ALV-induced erythroblastosis samples. The VB1 exon is located inside the 4.5-kb *Eco*RI fragment of the α allele (and the 2.3-kb fragment of the β allele). Thus, to determine whether ALV provirus insertion occurs in this region, the 4.5-kb *Eco*RI fragment of the α allele was subcloned and used as a probe (the R4.5 probe, Fig. 2*A*). The strategy of this experiment is illustrated in Fig. 2*A*. If the ALV proviral insertion occurs near VB1 as depicted, we should see an interruption of the *Eco*RI 4.5-kb fragment by the provirus, resulting in two fragments (X and Y) detectable with probe R4.5. Since there is an *Eco*RI site present in the ALV LTR, fragment X should contain a portion of the LTR, and fragment Y should contain the complementary part of the LTR. As a result, the sum of X and Y should be equal to 4.5 kb plus the size of an ALV LTR, which is 0.34 kb. Thus, one would anticipate seeing two altered fragments, with their sum being ≈4.8 kb. (This calculation was based on the α allele, but the same argument holds for the β allele, except that the sum should be 2.6 kb.) The following data (Fig. 2*B* and Table 1) clearly demonstrate that this is indeed the case. The left panel shows *Eco*RI-digested

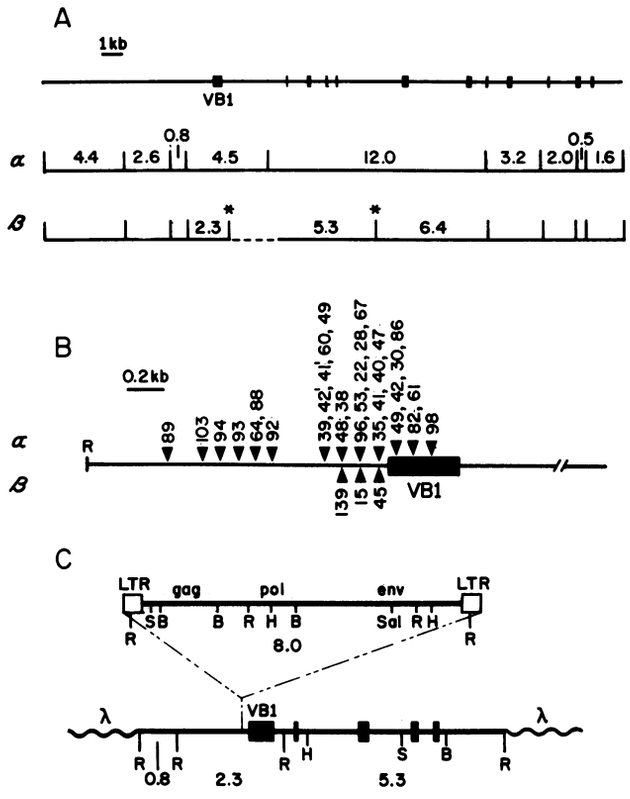

FIG. 1. (*A*) *Eco*RI restriction map of the α and β alleles of c-*erbB*. The α-allele map is according to that reported by Vennstrom and Bishop (10) and Sargeant *et al.* (15). The β-allele map was established by the isolation and restriction enzyme mapping of overlapping clones of this allele (data to be published elsewhere). Solid boxes show regions homologous to v-*erbB*. Size and approximate location of exons are based on previously reported heteroduplex analysis (10, 15). The location of the first exon homologous to v-*erbB*, designated VB1, is defined more accurately by fine restriction-enzyme mapping of the 4.5- and 2.3-kb *Eco*RI fragments. The vertical bars denote the *Eco*RI cleavage sites; ---, deleted sequences; *, *Eco*RI sites present only in the β allele. (*B*) Proviral integration sites in the c-*erbB* gene of erythroblastosis samples. Positioning of the integration sites in different samples (indicated by arrowhead with corresponding sample number) is based on the sizes of *Eco*RI restriction fragments as described in the text. The integration sites in α or in β are placed according to their relative distances from the 5′ *Eco*RI site of the 4.5- or 2.3-kb fragment, respectively. (*C*) Restriction enzyme map of clone λ139. Clone λ139 was isolated from a genomic library derived from leukemia sample 139. Restriction fragments were ordered based on their single- and double-digestion patterns as well as on their hybridization to specific cellular and viral probes. *Eco*RI, R; *Bam*HI, B; *Hin*dIII, H; *Sac* I, S; *Sal* I, Sal. The bottom line represents cellular sequences of the β allele. Solid boxes denote exon sequences. Wavy lines indicate the arms of the λ vector. Dotted line indicates the point of insertion of the ALV provirus (top line). LTRs are shown as boxes; gag, group-specific antigens; pol, polymerase; env, envelope glycoproteins.

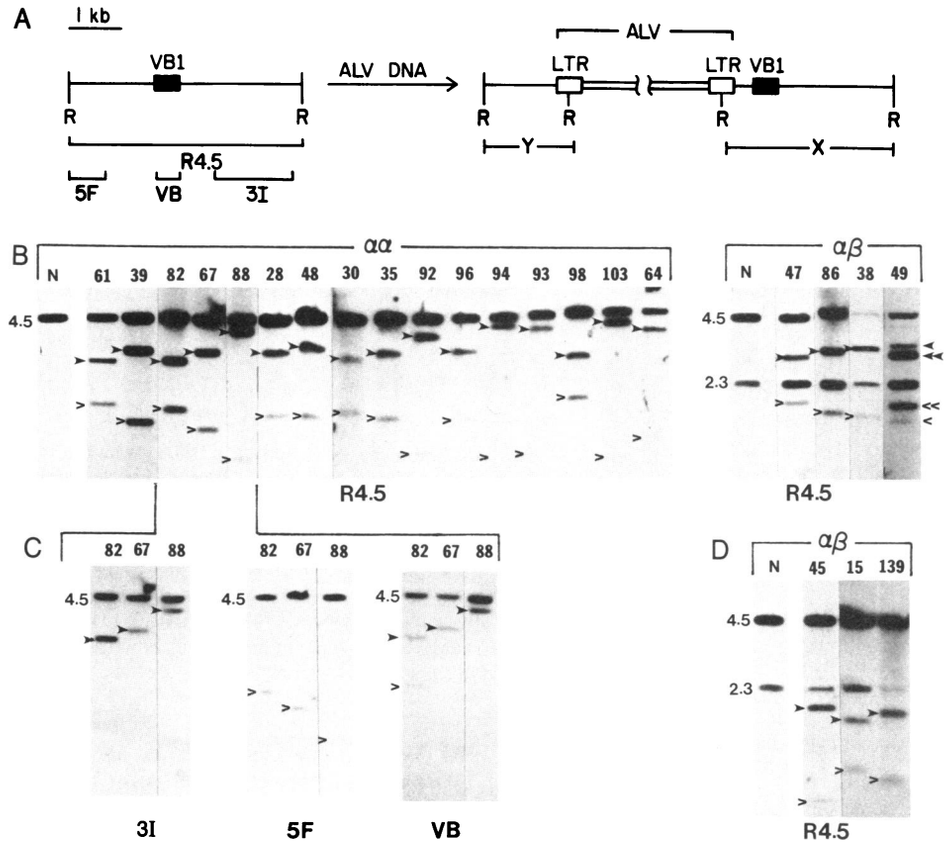

FIG. 2. *Eco*RI-digestion analysis of the proviral integration sites. (*A*) Schematic diagram of proviral insertion upstream from VB1. Also shown are probes used in this study, and the regions they detect. Probe R4.5 represents the 4.5-kb *Eco*RI fragment of the α allele. Probe 5F is a 0.8-kb *Eco*RI–*Pst* I fragment derived from the 5′ end of R4.5. Probe 3I is a 1.6-kb *Pvu* II fragment located in the 3′ intron region of R4.5. A 0.7-kb *Bam*HI–*Sac* I fragment specific for the 5′ end of v-*erbB* was used as the VB probe. This probe recognizes the 4.5- and 12.0-kb *Eco*RI fragments of the α allele (9); for clarity, only hybridization to the 4.5-kb fragment is included in *C*. (*B–D*) Southern blot analyses of *Eco*RI-digested DNA from normal uninfected (N) and erythroblastosis samples (numbers above lanes). Filters were hybridized with the probes indicated at the bottoms of the autoradiograms. Leukemia-specific bands that show rearrangements within the 4.5-kb *Eco*RI fragment (*B* and *C*) or the 2.3-kb *Eco*RI fragment (*D*) are indicated by solid or open arrowheads (X and Y fragments, respectively; see *A*). Sizes of the rearranged bands in *B* are summarized in Table 1. *B–D* are composites of five gels, among which the migration properties of the fragments differ slightly.

DNA samples from chicks of the αα type. In the normal control (lane N) probe R4.5 hybridizes to the 4.5-kb *Eco*RI fragment as expected. In other lanes with leukemic samples, two additional bands X (solid arrowheads) and Y (open arrowheads) can be identified (the larger fragments are arbitrarily designated X). In every case, X and Y total approximately 4.8 kb (Table 1).

Analysis of samples from chicks heterozygous for the α and β alleles are shown at right in Fig. 2*B*. The 4.5- and 2.3-kb fragments present in the normal control represent the α and β alleles, respectively. The panel shows samples in which alteration of the α allele is observed. Again, the sum of fragments X and Y is ≈4.8 kb. Sample 49 carries four rearranged fragments which pair into two sets of X and Y; presumably, this sample contains DNA from two clonal populations of leukemic cells, each harboring an ALV provirus near VB1 but at a slightly different site. It is noteworthy that the intensity of the 4.5-kb band is reduced relative to the 2.3-kb band in a few samples. Since these samples are from birds heterozygous for α and β, disruption of the α allele should correlate with the loss of the 4.5-kb band, assuming that all cells in the samples are transformed erythroblasts. Analysis of bone marrow samples that contain ≈80% erythroblasts (i.e., samples 38 and 49) does show significant reduction in the intensity of the 4.5-kb band relative to the 2.3-kb band. The residual 4.5-kb band is presumably derived from the undisrupted α allele present in the untransformed leukocytes in the bone marrow.

Table 1. Size of viral-cell junction fragments of proviruses inserted in the α allele

Sample	Fragment size, kb *Eco*RI	Fragment size, kb *Sac* I	Sample	Fragment size, kb *Eco*RI	Fragment size, kb *Sac* I
89	4.3, 0.5	12.0, 4.2	28	3.2, 1.6	10.5, 5.3
103	4.1, 0.7	11.0, 4.1*	22	3.2, 1.6	ND
94	4.0, 0.7	12.0, 4.2	53	3.1, 1.6	11.5, 5.3
93	4.0, 0.7	11.0, 4.3*	96	3.3, 1.6	11.0, 5.3
64	3.7, 1.0	12.0, 4.5	35	3.2, 1.7	11.0, 5.2
88	3.8, 1.0	11.5, 4.7	41	3.2, 1.7	ND
92	3.6, 1.1	11.5, 4.6	40	3.1, 1.7	10.5, 5.4
49	3.4, 1.4	11.5, 4.8	47	3.1, 1.7	10.5, 5.4
60	3.4, 1.4	9.6, 4.1*	49	3.0, 1.8	10.6, 5.3
41′	3.4, 1.4	11.8, 4.6	42	3.0, 1.8†	10.5, 5.4
42′	3.3, 1.4	10.5, 5.2	30	3.0, 1.8†	10.2, 5.4
39	3.4, 1.4	11.0, 5.0	86	3.0, 1.8†	10.5, 5.5
38	3.3, 1.5	11.0, 5.2	82	3.0, 1.9†	ND
48	3.4, 1.5	10.5, 5.2	61	3.0, 1.9†	11.0, 5.5
67	3.3, 1.6	11.0, 5.3	98	2.8, 2.0†	10.8, 5.4

Shown are the 30 typical cases in which direct proviral insertions into the α allele were found. Cases involving the processed *erbB* gene (see *Discussion*) and the proviral insertions in the β allele are not included. *Eco*RI and *Sac* I junction fragments are determined as described for Figs. 2 and 3, respectively. Samples are arranged in order of their integration sites relative to VB1. ND, not determined.
*Deleted provirus.
†Integration site within VB1.

The experiment described above indicates that there is a high frequency of proviral integrations near the VB1 exon and in the *Eco*RI fragment, but it does not reveal whether the proviral integration sites are located upstream or downstream from the VB1 exon. To examine this, we hybridized the same DNA blot as in Fig. 2*B* to the following region-specific probes (see Fig. 2*A*): 5F (the 5′ flanking sequence), 3I (3′ intron), and VB (v-*erbB*). Examples of such hybridizations are shown in Fig. 2*C*; probe 3I detects exclusively the longer (X) fragment, whereas probe 5F hybridizes more strongly to the shorter (Y) fragments. This indicates that the interruption due to proviral insertion is in the 5′ half of the *Eco*RI 4.5-kb fragment. Hybridization with probe VB detects only fragment X in most cases, as shown for samples 67 and 88. This result suggests that VB1 is linked to its downstream intron sequence, implying that the ALV provirus must integrate on the 5′ side of VB1. In sample 82, both frag-

ments X and Y are detected by probe VB, suggesting that, in this case, the ALV provirus is integrated within VB1. Based on the sizes of fragment X (or Y) and the information regarding their relative positions to VB1, the individual proviral integration sites can be determined. They are summarized in Fig. 1*B*. It is apparent that the ALV proviral integration sites are clustered in a region immediately upstream from VB1. In those cases (e.g., sample 82) where proviral integration within VB1 is suspected, the sizes of fragments X and Y match very well with what is predicted if there is a disruption inside VB1. Based on these data, we conclude that in erythroblastosis samples, the ALV provirus preferentially integrates just 5′ to or within the region where homology to v-*erbB* starts.

Activation of the β Allele by ALV Proviral Insertion. Having found that the α allele is frequently mutated by proviral insertion near VB1, we were interested in determining whether the β allele could be interrupted similarly. Using the strategy described above, we were able to show for three αβ heterozygous samples that insertion near the β allele occurs. As shown in Fig. 2*D*, the sum of X and Y in these cases equals 2.6 kb (as opposed to 4.8 kb for the α allele). In addition, the intensity of the unaltered β 2.3-kb band is largely reduced compared to that of the unaltered α 4.5-kb band. The locations of the three integration sites relative to VB1 map to the same region as those for the α allele (Fig. 1*B*). Since the alterations in the β allele are the only ones detectable in these leukemia samples, the data indicate that insertional activation of the β allele can also induce erythroblastosis.

To conclusively document that ALV proviral insertion indeed occurs in the β allele, we have isolated a c-*erbB* clone, λ139, from a genomic library of partially *Eco*RI-digested DNA from leukemia sample 139. This clone carries a 16.4-kb insert. A battery of enzymes was used to construct a restriction map, which is summarized in Fig. 1*C*. The map is in complete agreement with the insertion of an intact ALV provirus in the 2.3-kb *Eco*RI fragment of the β allele, with the provirus oriented in the same transcriptional direction as the c-*erbB* gene. That the ALV provirus is intact was further substantiated by *in vitro* transfection of chicken embryo fibroblasts with the λ139 DNA, resulting in the release of infectious virus (unpublished data). The integration site of the provirus fits exactly that determined by the Southern analysis [Fig. 2*D* (lane 139) and Fig. 1*B*].

The Structure and the Orientation of the Provirus. The finding that an intact ALV provirus is present near the c-*erbB* gene deviates from the previous observations that the ALV proviruses linked to the c-*myc* gene in B-lymphomas frequently show large deletions, especially near and including the 5′ LTR (4–6). It was postulated that active transcription of an upstream promoter (in this case, the 5′ LTR) may significantly affect the strength of the downstream promoter (3′ LTR)—a phenomenon described as promoter occlusion (16, 17). Therefore, removal of the 5′ LTR appears to be necessary for efficient utilization of the 3′ LTR for downstream promotion of the oncogene. It was therefore of interest to find that λ139 carries a full-length ALV provirus. To see whether this is generally true for other leukemic-cell DNA, *Sac* I digestion was conducted. As shown in Fig. 3, *Sac* I has a single cleavage site near the 5′ terminus of ALV DNA. The *Sac* I map of c-*erbB* surrounding the proviral integration sites is also shown. For the undisrupted α allele, probe R4.5 should detect two fragments, 8.0 and 3.5 kb long. Upon proviral integration, the 8.0-kb fragment is disrupted into two fragments, due to the presence of the additional *Sac* I site in ALV DNA. If the provirus is full-length (8 kb), the sum of the two new *Sac* I fragments should approximate 8.0 + 8.0, or 16.0 kb. This appears to be the case for the majority of the leukemic samples (Fig. 3 and Table 1). It is also noteworthy that *Eco*RI digestion analysis presented above indicates that both LTRs might be intact, since the *Eco*RI sites of the LTRs appear to be present in all cases. Although rigorous proof that the proviruses are intact has to come from transfection studies such as those described above for λ139 clone, the preponderance of full-sized proviruses in erythroblastosis samples indicates that the presence of an intact provirus may not be unique to the DNA of sample 139. This data suggests that promoter occlusion, if it occurs in this case, is not absolute and that its effect is not sufficient to block the activation of c-*erbB* by a 3′ LTR. Alternatively, the provirus may utilize the 5′ LTR as the promoter to activate the c-*erbB* gene.

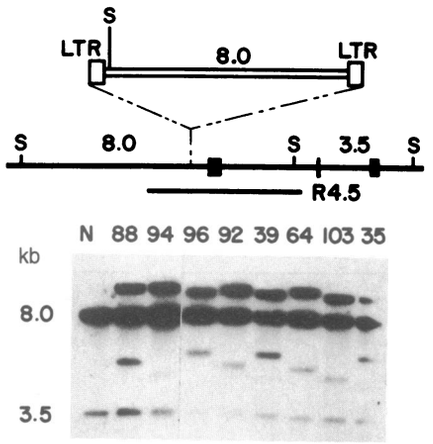

FIG. 3. *Sac* I digestion analysis of proviral DNA structure. (*Upper*) *Sac* I (S) restriction map of an intact ALV provirus integrated 5′ to VB1 and in the same transcriptional orientation as the α allele. Solid boxes represent exons. Sizes of the full-length provirus and the two *Sac* I fragments of the uninterrupted allele are given (in kb) above the provirus diagram and the restriction map, respectively. The region detectable by R4.5 is shown. (*Lower*) Southern hybridization of *Sac* I-digested normal (N) and erythroblastosis DNA with R4.5 probe. Erythroblastosis sample numbers are above lanes. The sizes of the rearranged bands in leukemia samples are listed in Table 1.

Sac I analysis also provides important information regarding the orientation of the proviruses. For example, sample 88 gives two *Sac* I, viral-cell junction fragments of about 11.5 and 4.7 kb. The relative intensity of the two bands suggests that the 11.5-kb band is the downstream fragment and the 4.7-kb band, the upstream one. Hybridization to probe 3I (Fig. 2) invariably detects the larger of the two tumor-specific bands, confirming this assignment (data not shown). We know from the data in Table 1 the sizes of the *Eco*RI junction fragments and, hence, the location of the integrated provirus (Fig. 1*B*). These data together allow the viral *Sac* I site to be unambiguously placed near the 5′ end of the inserted provirus; the provirus therefore is oriented in the same transcriptional direction as c-*erbB*. The calculated distances from the viral *Sac* I site to the LTRs agree very well with the intact ALV map, further confirming this alignment. All the proviruses surveyed by *Sac* I analysis in this study are oriented in the same direction as c-*erbB*.

DISCUSSION

The studies described here suggest that ALV activates c-*erbB* in erythroblastosis by a mechanism very similar to its activation of c-*myc* in B-lymphomas: the proviruses are oriented in the same transcriptional direction as the host oncogene and are clustered either at or immediately 5′ to a region (≈1.5 kb) corresponding to the start of the viral oncogene. Although exceptions to this general activation scheme exist

(7), this mechanism, referred to as promoter insertion, represents the predominant one used by the ALV provirus. Reticuloendotheliosis virus, another avian retrovirus, also uses promoter insertion as the major mechanism of c-*myc* activation in B-lymphomas caused by this virus (ref. 18 and unpublished results). In contrast, almost all the proviruses in mouse mammary tumor virus-induced mammary carcinomas are arranged either in the opposite orientation or downstream from the putative oncogene. Furthermore, the integration sites are spread over a large (20-kb) region (19). In this case, presumably, the LTR enhancer is involved in activation. Clearly, in different systems, different activation mechanisms are favored. What dictates the mode of viral integration as well as oncogene activation is unclear, but it may be related to the intrinsic properties of the virus (e.g., the strengths of the enhancer and promoter), the oncogene in question (the local conformation and the structural requirements for activation), or a combination of both. In the case of c-*myc* activation, most of the ALV and reticuloendotheliosis virus DNA integrations result in truncation of the c-*myc* transcript and removal of the first noncoding exon (ref. 20 and unpublished results). It was postulated that the first noncoding exon may contain a negative-controlling element that inhibits either the transcription or translation of the gene (20–22). The situation with c-*erbB* is less clear, since the coding capacity of the gene has not been defined fully. However, recent evidence strongly suggests that the c-*erbB* product is closely related or identical to the epidermal growth factor (EGF) receptor (23–25). Since the region of homology involves the carboxyl-terminal portion of the EGF receptor and v-*erbB*, one would expect the c-*erbB* coding sequences to extend significantly further upstream from VB1, where the proviral integration sites are concentrated. All the activated c-*erbB* products would, therefore, represent truncated versions of the normal protein. It is, then, interesting that the starting points of all the activated c-*erbB* genes studied here map very close to the point of insertion of v-*erbB* sequences in AEV_R and AEV_H. This suggests that interruption in this region of c-*erbB* probably is important for activation. The requirement to interrupt the c-*erbB* locus and generate a truncated product perhaps also imposes a need for the promoter-insertion (as opposed to enhancer-insertion) type of proviral activation, since, in this region, no cellular promoter is present to be activated by the LTR enhancer.

Whether c-*erbB* is identical to EGF receptor or not, the chicken c-*erbB* locus is a complex one; the region homologous to v-*erbB* spans more than 20 kb and contains at least 12 exons. Added to this complexity is the presence of structural polymorphisms in different lines of chickens. Using cloning and hybridization studies, we have identified a second allele, β, which differs from the previously known allele, α, primarily by a deletion in the intron region. The α and β alleles can account for the majority but not all of the polymorphic *erbB* elements observed in chickens and must constitute the major c-*erbB* locus, since we have not found any chickens that lack both alleles. Among the few $\alpha\beta$ heterozygotes studied, the β allele appears to be as susceptible to proviral insertion as the α allele (3/7 vs. 4/7; Fig. 3 *A* and *B*).

The present communication is primarily concerned with the typical promoter-insertion mechanism of c-*erbB* activation, which accounts for 90% (34/38) of the cases examined. We previously reported an atypical case where a single altered c-*erbB* fragment contains an LTR and v-*erbB* related exons but no intron sequences, as if the activated c-*erbB* message had been reverse-transcribed and reinserted into the host genome (9). We have again observed this phenomenon in the present study; the altered c-*erbB* fragment of the four remaining cases possesses these features (unpublished data). One such fragment was cloned, and structural analysis confirms the processed nature of the *erbB* gene. The linkage point between the provirus and the processed *erbB* gene again maps near VB1. The generation of such a processed gene can occur either intracellularly, as has been suggested for the formation of other pseudogenes (26), or via virus intermediate (ref. 27 and H. Robinson, personal communications). In either case, promoter-insertion probably was involved in the initial activation of the oncogene (4, 5). When we include these cases in the category of promoter-insertion activation, we find a striking statistic for c-*erbB* activation: In the 37 chicks with erythroblastosis (38 proviruses) analyzed, there is a 100% correlation between c-*erbB* alteration and erythroblastosis development. Furthermore, virtually all proviruses found linked to c-*erbB* are clustered in a small chromosomal region and are uniformly aligned in a configuration compatible with the promoter-insertion type of activation.

We thank J. Vitkuske and R. Wagner for excellent technical assistance; J. Dodgson, S. Conrad, and M. Fluck for critical reviews of the manuscript; and T. Vollmer for assistance in manuscript preparation. This work was supported in part by a grant from the Leukemia Research Foundation and by Grant CA33158 from the National Cancer Institute. H.-J.K. gratefully acknowledges support from the Faculty Research Award of the American Cancer Society.

1. Weiss, R. A., Teich, N. M., Varmus, H. E. & Coffin, J. M. (1982) *Molecular Biology of Tumor Virus* (Cold Spring Harbor Laboratory, Cold Spring Harbor, NY).
2. Crittenden, L. B. & Kung, H. J. (1983) in *Mechanisms of Viral Leukemogenesis*, eds. Goldman, J. M. & Jarret, O. (Churchill-Livingstone, Edinburgh, Scotland), pp. 64–88.
3. Hayward, W. S., Neel, B. G. & Astrin, S. M. (1981) *Nature (London)* **290**, 475–480.
4. Payne, G. S., Courtneidge, S. A., Crittenden, L. B., Fadly, A. M., Bishop, J. M. & Varmus, H. E. (1981) *Cell* **23**, 311–322.
5. Neel, B. G., Hayward, W. S., Robinson, H. L., Fang, J. & Astrin, S. M. (1981) *Cell* **23**, 323–334.
6. Fung, Y.-K., Fadly, A. M., Crittenden, L. B. & Kung, H. J. (1981) *Proc. Natl. Acad. Sci. USA* **78**, 3418–3422.
7. Payne, G. S., Bishop, J. M. & Varmus, H. E. (1982) *Nature (London)* **295**, 209–213.
8. Fung, Y.-K., Crittenden, L. B. & Kung, H. J. (1982) *J. Virol.* **44**, 742–746.
9. Fung, Y.-K., Lewis, W. G., Crittenden, L. B. & Kung, H. J. (1983) *Cell* **33**, 357–368.
10. Vennstrom, B. & Bishop, J. M. (1982) *Cell* **28**, 135–143.
11. Maniatis, T., Fritsch, E. & Sambrook, J. (1982) *Molecular Cloning: A Laboratory Manual* (Cold Spring Harbor Laboratory, Cold Spring Harbor, NY).
12. Murray, N. E. (1983) in *Lambda II*, eds. Hendrix, R. W., Roberts, J. W., Stahl, F. W. & Weisberg, R. A. (Cold Spring Harbor Laboratory, Cold Spring Harbor, NY), pp. 395–432.
13. Hohn, B. & Murray, K. (1977) *Proc. Natl. Acad. Sci. USA* **74**, 3259–3263.
14. Southern, E. M. (1975) *J. Mol. Biol.* **98**, 503–517.
15. Sargeant, A., Sanle, S., Leprince, D., Begue, A., Rommens, G. & Stehelin, D. (1982) *EMBO J.* **1**, 237–242.
16. Adhya, S. & Gottesman, M. (1982) *Cell* **29**, 939–944.
17. Cullen, B. R., Lomedico, P. T. & Ju, G. (1984) *Nature (London)* **307**, 241–245.
18. Noori-Daloii, M. R., Swift, R. A., Kung, H.-J., Crittenden, L. B. & Witter, R. L. (1981) *Nature (London)* **294**, 574–576.
19. Nusse, R., VanOoyen, A., Cox, D., Fung, Y. & Varmus, H. E. (1984) *Nature (London)* **307**, 131–136.
20. Shih, C.-K., Linial, M., Goodnow, M. M. & Hayward, W. S. (1984) *Proc. Natl. Acad. Sci. USA* **81**, 4697–4701.
21. Saito, H., Hayday, A. C., Wiman, K., Hayward, W. S. & Tonegawa, S. (1983) *Proc. Natl. Acad. Sci. USA* **80**, 7476–7480.
22. Taub, R., Moulding, C., Battey, J., Murphy, W., Vasicek, T., Lenior, G. & Leder, P. (1984) *Cell* **36**, 339–348.
23. Donward, J., Yarden, Y., Mayes, E., Scrao, G., Totty, N., Stockwell, P., Ulnich, A., Schlessinger, J. & Waterfield, M. D. (1984) *Nature (London)* **307**, 521–527.
24. Merlino, G. T., Xu, Y.-H., Ishii, W., Clark, A. J., Semba, K., Tooshima, K., Yamamota, T. & Pastan, I. (1984) *Science* **224**, 417–419.
25. Lin, C. R., Chen, W. S., Kruiger, W., Stolarsky, L. S., Weber, W., Evans, R. M., Verma, I. M., Gill, G. N. & Rosenfeld, M. G. (1984) *Science* **224**, 843–848.
26. Sharp, P. A. (1983) *Nature (London)* **301**, 471–472.
27. Bishop, J. M. (1983) *Annu. Rev. Biochem.* **52**, 301–354.